



HAL
open science

High-order sliding mode control of a doubly salient permanent magnet machine driving marine current turbine

Hao Chen, Shifeng Tang, Jingang Han, Tianhao Tang, Nadia Aït-Ahmed, Zhibin Zhou, Mohamed Benbouzid

► To cite this version:

Hao Chen, Shifeng Tang, Jingang Han, Tianhao Tang, Nadia Aït-Ahmed, et al.. High-order sliding mode control of a doubly salient permanent magnet machine driving marine current turbine. *Journal of Ocean Engineering and Science*, 2021, 6 (1), pp.12-20. 10.1016/j.joes.2020.04.001 . hal-03463388

HAL Id: hal-03463388

<https://hal.science/hal-03463388>

Submitted on 2 Dec 2021

HAL is a multi-disciplinary open access archive for the deposit and dissemination of scientific research documents, whether they are published or not. The documents may come from teaching and research institutions in France or abroad, or from public or private research centers.

L'archive ouverte pluridisciplinaire **HAL**, est destinée au dépôt et à la diffusion de documents scientifiques de niveau recherche, publiés ou non, émanant des établissements d'enseignement et de recherche français ou étrangers, des laboratoires publics ou privés.

Journal Pre-proof

High-order sliding mode control of a doubly salient permanent magnet machine driving marine current turbine

Hao Chen , Shifeng Tang , Jingang Han , Tianhao Tang ,
Nadia Ait-Ahmed , Zhibin Zhou , Mohamed Benbouzid

PII: S2468-0133(20)30031-0
DOI: <https://doi.org/10.1016/j.joes.2020.04.001>
Reference: JOES 170



To appear in: *Journal of Ocean Engineering and Science*

Received date: 31 October 2019
Revised date: 14 February 2020
Accepted date: 7 April 2020

Please cite this article as: Hao Chen , Shifeng Tang , Jingang Han , Tianhao Tang ,
Nadia Ait-Ahmed , Zhibin Zhou , Mohamed Benbouzid , High-order sliding mode control of a doubly salient permanent magnet machine driving marine current turbine, *Journal of Ocean Engineering and Science* (2020), doi: <https://doi.org/10.1016/j.joes.2020.04.001>

This is a PDF file of an article that has undergone enhancements after acceptance, such as the addition of a cover page and metadata, and formatting for readability, but it is not yet the definitive version of record. This version will undergo additional copyediting, typesetting and review before it is published in its final form, but we are providing this version to give early visibility of the article. Please note that, during the production process, errors may be discovered which could affect the content, and all legal disclaimers that apply to the journal pertain.

© 2020 Published by Elsevier B.V. on behalf of Shanghai Jiaotong University.
This is an open access article under the CC BY-NC-ND license.
(<http://creativecommons.org/licenses/by-nc-nd/4.0/>)

Highlights:

- The low speed stator-permanent magnet machine with toothed pole has extraordinary advantages for marine current power generation
- The machine is a strongly coupled nonlinear system with torque ripple, but the sliding mode control (SMC) can well meet the control requirements
- Compared with the traditional controller (FOSMC), the proposed controller (HOSMC) can greatly reduce chattering and has strong robustness
- The stability of the controller based on super-twisting algorithm (HOSMC) is proved, and the results demonstrate convincingly the effectiveness of the proposed controller (HOSMC)

Journal Pre-proof

High-order sliding mode control of a doubly salient permanent magnet machine driving marine current turbine

Hao Chen^{a,*}, Shifeng Tang^a, Jingang Han^a, Tianhao Tang^a, Nadia Ait-Ahmed^b, Zhibin Zhou^c, Mohamed Benbouzid^{a,d}

^a The Institute of Power Drive and Control, Shanghai Maritime University, 201306, Shanghai, China

^b Institut de Recherche en Energie Electrique de Nantes Atlantique, University of Nantes, 44602, Saint-Nazaire, France

^c ISEN Yncréa Ouest, University of Brest, FRE CNRS 3744 IRDL, 29200, Brest, France

^d University of Brest, UMR CNRS 6027 IRDL, 29238, Brest, France

Abstract: Due to the harsh and changeable marine environment, one low speed stator-permanent magnet machine named doubly salient permanent magnet machine with toothed pole is applied for marine current energy conversion system. Indeed, this machine has simple structure, intriguing fault tolerance, and higher power density, which could adequately satisfy the different complicated operation conditions. However, its permanent magnet flux-linkage has the same variation period as the inductance which leads to a strong nonlinear coupling system. Moreover, the torque ripple caused by this special characteristics, uncertainty of system parameters and disturbance of load greatly increases the difficulty of control in this strongly coupling system. Consequently, the classical linear PI controller is difficult to meet the system requirement. In this paper, the high-order sliding mode control strategy based on the super-twisting algorithm for this system is creatively utilized for the first time. The stability of the system within a limited time is also proved with a quadratic Lyapunov function. The relative simulation results demonstrate convincingly that, the high-order sliding mode control has little chattering, high control accuracy and strong robustness.

Keywords: Doubly salient permanent magnet machine, Torque ripple, Chattering, High-order sliding mode control, Super-twisting algorithm

*Corresponding author at: The Research Institute of Power Drive and Control, Shanghai Maritime University, 201306, Shanghai, China. Tel.: +86 177 0160 3266;
E-mail address: chen hao@shmtu.edu.cn

1. INTRODUCTION

In recent years, the fossil energy is gradually exhausted due to the acceleration of the global industrialization process. Meanwhile, the environmental pollution caused by the extensive use of fossil energy becomes more and more serious. Consequently, the renewable energy has attracted widespread attention during the past decades. Nowadays, both the efficiency and dependability of the renewable energy technologies have been continuously enhanced [1]-[4]. According to the statistics, the estimated renewable energy accounted for 24.5% of the global generation of electricity by the end of 2017, while this value approximately reached up to 26.5% in 2018 [5]. Among the various renewable energies, ocean energy becomes more and more interesting due to its abundant energy reserves. Unfortunately, among various forms of ocean energy, only marine current energy appears the enormous commercial value considering its high energy density, strong predictability and similar technologies to the mature Wind Energy Conversion System (WECS) [6][7]. Even for the marine current energy, there is approximated 50 GW or 180 TWh annually of the economically exploitable resource worldwide [1]. Thus, the utilization of the marine current energy will certainly mitigate the energy crisis to a certain extent.

The generator, the main component of Marine Current Energy Conversion System (MCECS) to transform the mechanical energy into the electrical energy, must be considered cautiously. Normally, the low marine current speed results in relatively low rotation speed of the turbine. An external gearbox is always demanded to achieve relative high machine rotor speed. However, it will inevitably bring the relative high failure rate and increase the difficulties of the maintenance in the harsh working environment. Consequently, the direct drive MCECS with low speed machine is preferred [8]. The application of the conventional generators such as Permanent Magnet Generator (PMG), Induction Generator (IG) and Doubly-Fed Induction Generator

(DFIG) has been greatly limited in virtue of this reason. In this paper, one low speed stator-Permanent Magnet (PM) machine: toothed pole Doubly Salient Permanent Magnet (DSPM) machine (50 rpm, 10 kW) is proposed. This kind machine employs the magnets in the stator and can decouple of the frequency from the pole pair [9]. In addition, the forward, reverse and four-quadrant operation of this machine can be easily realized by changing the order of the inverter conduction phase and the sense of winding current. Accordingly, the DSPM machine is quite suitable for the frequent start-stop, acceleration and deceleration occasions including marine current power generation and ship propulsion.

However, due to its special structure, the back-EMF has the same variation as the inductance which would bring big torque ripple even with conventional sinusoidal current waveform. This torque ripple would degrade the performance of the transmission system and even cause the shafting oscillation to endanger the mechanical device. Moreover, this toothed pole DSPM machine is difficult to control by the conventional linear controllers because of the nonlinear dynamic model. Therefore, it is of great significance to study the current waveform and corresponding control methods of this special machine.. In Ref. [10], the causes of torque ripple are firstly analyzed in detail; then, the switching angle adjustment method and rotor skew slot technology are proposed to reduce the ripple. Nevertheless, this control method needs to confirm the conduction angle which will make the control mode more complex. The skew technology needs to change the structure of the machine which increases the cost. In Ref. [11], the maximum torque and torque pulsation are reduced by optimizing the turn-on and turn-off angles and reducing the number of conducting phases. However, the output torque is also reduced. In Ref. [12] and Ref. [13], they propose the forward commutation method. This method can reduce the commutation torque ripple by changing the current rising time. Nevertheless, the advance

angle is not easy to determine. In Ref. [14], a variable parameter PI controller based on a single-chip TMS320F28335 is proposed. The current loop, as well as the voltage loop, employs **gain-scheduled** PI controller based on the linearized model of the DSPM machine. Unfortunately, this simplified linear system cannot achieve precise control results. In Ref. [9] and Ref. [15], they propose one complex quasi-sinusoidal current waveform to diminish the torque ripple and one First-Order Sliding Mode Control (FOSMC) to deal with the nonlinear model. **However, the mathematical current formula highly depends on the parameters of the DSPM machine. Meanwhile, FOSMC will undoubtedly bring the chattering which may also bring the torque ripple. Actually, the chattering is the inherent phenomenon of Sliding Mode Control (SMC) and is mainly due to the the discontinuous switch character in essence of this control.**

For the sake of decreasing the torque ripple and increasing the robustness, one High-Order Sliding Mode Control (HOSMC) strategy based on **Super-Twisting Algorithm (STA)** is adopted for this toothed pole DSPM machine-based MCECS in this **paper**. This paper is structured as follows: the partially typical model of MCECS is established in section 2, including the **marine current** resource, turbine and DSPM machine; in section 3, HOSMC strategy based on STA, which has great robustness and convergence rapidity, is introduced and optimized for the DSPM machine; subsequently, a quadratic Lyapunov function is used to prove stability of the whole control system within a limited time; section 4 deals with the simulation and analysis in different situations; **eventually**, a conclusion is given in section 5.

2. MARINE CURRENT TURBINE MODELING

The global scheme of MCECS is very similar with that of WECS. Ordinarily, the global scheme of MCECS contains some essential components: the resource, the marine turbine, the generator, the transformer and the grid-connected converter (Fig. 1). When the turbine blades are driven by the marine current, a lift perpendicular to the direction

of the flow is produced. This continuous force makes the turbine rotate. Subsequently, the generator is driven by the mechanical transmission structure and generates electricity under the control of the inverter.

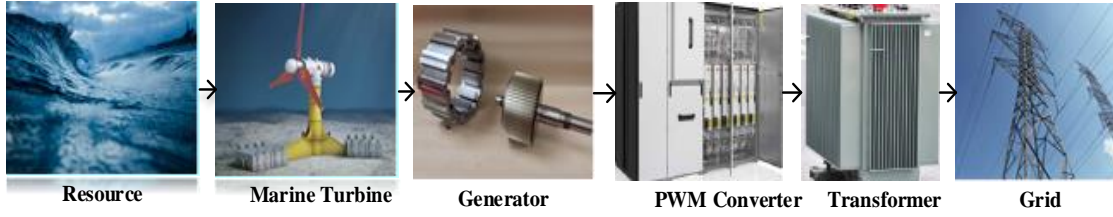


Fig. 1. Global scheme of MCECS [16][17].

For the MCECS, an appropriate model for the marine current resources is required firstly. Many researchers have developed several different models of the marine current speed to assess their potential energy. One first-order model provided by SHOM (Service Hydrographique et Océanographique de la Marine, France) is adopted in this part due to the remarkable reliability and simplicity [18]. The tidal current velocity V_{tide} is given by Eq. (1).

$$V_{tide} = V_{nt} + \frac{(C-45)(V_{st}-V_{nt})}{95-45} \quad (1)$$

Where: C is the tide coefficient; 95 and 45 are mean spring tide and neap tide medium coefficients according to experimental research respectively; V_{nt} and V_{st} are the hourly intervals neap and spring tide current velocities.

According to the model above, the marine current velocity data in Penmarc'h, France is shown in Fig. 2. From this figure, the maximum value of the absolute velocity of flow does not exceed 3.5m/s. The available mechanical power P_{mec} of the marine current turbine, extracted from the fluid is expressed by the following Eq. (2) [19][20].

$$P_{mec} = C_p P_{hyd} = \frac{1}{2} C_p \rho A V_{tide}^3 \quad (2)$$

Where: P_{hyd} is the hydrodynamic power; ρ is the density of the ocean (1024 kg/m^3); A is the cross section of the turbine (m^2); V_{tide} is the current velocity (m/s); C_p is the power coefficient.

In order to meet nominal operation condition, the **power coefficient** C_p of marine current turbine is limited with the restriction as Eq. (3)[15].

$$C_p = \frac{2P_{mec}\omega_m^2}{\rho\pi\lambda^2V_{tide}^5} = \frac{2P_{hyd}\omega_m^2}{\rho\pi(1-\eta)\lambda^2V_{tide}^5} \quad (3)$$

Where: λ is the Tip Speed Ratio; η is the system mechanical losses percentage; ω_m is the mechanical speed (rad/s).

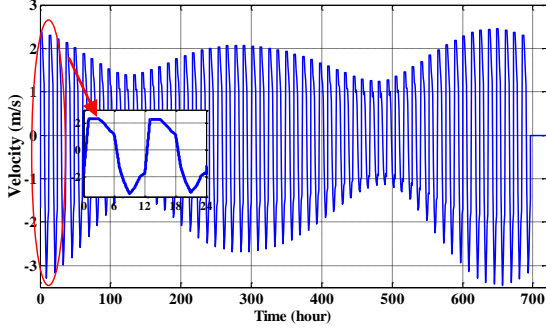


Fig. 2. Marine current velocity.

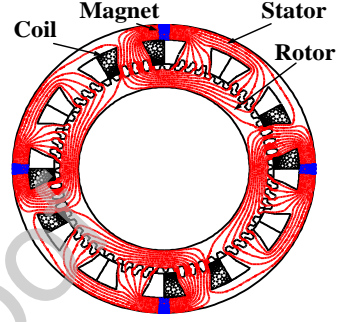


Fig. 3. DSPM machine structure.

As described in the introduction, this toothed pole DSPM machine is accepted by MCECS due to its prominent advantages and **simple** maintenance considerations. This machine **has been already** designed and optimized to achieve the maximum volume torque, **with a maximum torque of 45.5 kNm/m³**. The stator of this machine has four non-rotating PM, 48 teeth and 12 slots; while the rotor only contains 64 teeth [21]. Some more details of this DSPM machine design can be found in Ref. [22]. The simplified structure of this DSPM machine is shown in Fig. 3.

Actually, the establishment of the dynamic mathematical model needs to consider a number of factors. According to the previous model analysis in Ref. [23], some assumptions are required to simplify the analysis. A dynamic park model of the DSPM machine in d-q frame is derived with the Concordia and Park transformations and presented in the following Eqs. (4)-(6) [15].

$$\begin{cases} \varphi_d = -L_d i_d - M_{dq} i_q - \sqrt{\frac{3}{2}} \varphi_1 \\ \varphi_q = -L_q i_q - M_{dq} i_d \end{cases} \quad (4)$$

$$\begin{cases} v_d = -(R_s + 2\omega_e M_{dq})i_d + \omega_e \left(\frac{3L_d}{2} - \frac{L_q}{2}\right)i_q - L_d \frac{di_d}{dt} - M_{dq} \frac{di_q}{dt} \\ v_q = -(R_s - 2\omega_e M_{dq})i_q - \omega_e \left(\frac{3L_q}{2} - \frac{L_d}{2}\right)i_d - L_q \frac{di_q}{dt} - M_{dq} \frac{di_d}{dt} \end{cases} \quad (5)$$

$$\begin{cases} J_m \frac{d\omega_m}{dt} = T_{em} - T_m - f \omega_m \\ P_m + P_{em} = J_m \omega_m \frac{d\omega_m}{dt} + f \omega_m^2 \end{cases} \quad (6)$$

Where: $L_{d,q}$ represents the model of stator inductance based on d-q coordinate; M_{dq} is the mutual inductance; T_m and T_{em} are mechanical torque and electromagnetic torque; θ_e is the electrical angle; ω_e is the electrical angular velocity; J_m and f are rotary inertia and viscosity coefficient, respectively; N_r is the number of rotor teeth.

$$L_{d,q} = L_0 - M_0 \pm \left(\frac{L_1}{2} + M_1\right) \cos 3\theta_e \quad (7.a)$$

$$M_{dq} = -\left(\frac{L_1}{2} + M_1\right) \sin 3\theta_e \quad (7.b)$$

$$T_{em} = -\sqrt{\frac{3}{2}} N_r \varphi_1 i_q + \frac{N_r}{2} (L_d - L_q) i_d i_q - \frac{N_r}{2} M_{dq} (i_d^2 - i_q^2) \quad (7.c)$$

$$\theta_e = \int \omega_e dt, \quad \omega_m = \frac{\omega_e}{N_r} = \frac{2\pi f}{N_r} \quad (7.d)$$

3. CONTROL STRATEGIES

It is generally true that the classical linear controllers including the PI and PID are very suitable for the linear time-invariant system. However, as for this toothed pole DSPM machine, it is a typical non-linear system. Even for the **sinusoidal current waveform**, the PI controllers cannot effectively make the speed and current tracking error within the allowable range. Moreover, for the appropriate current waveform which contains certain harmonics to reduce the torque ripple, it would undoubtedly make the input complicated and increase the difficulties in control [9] [15]. Furthermore, the system usually **needs to** operate at different states with variable input and load due to the harsh underwater working environment. Consequently, a robust controller is **extremely beneficial to** these problems. **It is recognized that SMC is a prominent**

method of nonlinear control. It is widely used in many fields owing to its great robustness and fast convergence to external interference and internal parameter variations.

3.1 Introduction of HOSMC

Essentially, the principle of SMC is to force the trajectories of desired plant states onto some predesigned sliding surfaces by discontinuous controls. FOSMC is intensely easy to design and possesses certain robust performance. However, the application of FOSMC is hindered by the chattering phenomenon due to the multifarious inertia, which might lead to high-frequency vibration of the system. Thus, HOSMC appears subsequently. According to the theory proposed by Arie Levant, the sliding set $s = \dot{s} = \ddot{s} = \dots = s^{(r-1)} = 0$ on sliding mode surface $s(t, x) = 0$ is non-empty and consists of Filippov trajectories of discontinuous dynamic systems. Then, the relevant motion satisfying this condition is called the “ r -order sliding mode” with respect to the sliding mode surface ($r \geq 2$). HOSMC extends the idea of traditional sliding mode. It does not apply the discontinuous control variable to the first derivative of the sliding modulus, but applies it to the higher-order derivative. This not only retains the advantages of FOSMC, but also significantly reduces chattering [24]. At present, the Second-Order Sliding Mode Control (SOSMC) is widely accepted and supported by the theory [27]-[28]. Moreover, it is the most frequently applied HOSMC which has simple structure and little requirement of target information. In order to establish the controller based on HOSMC appropriately, the modeling process is explained by the following content.

By treating the DSPM machine control system as a controlled dynamic system, the control objectives can be handled more easily.. The state equation of a single input nonlinear dynamic system is defined as the Eq. (8).

$$\begin{cases} \dot{x} = f(x, t) + g(x, t)u \\ y = s(x, t) \end{cases} \quad (8)$$

Where: x is the system state variables; u is the control input; $f(x, t)$ and $g(x, t)$ are both smooth uncertain continuous functions.

It is worthwhile to design a suitable sliding surface, which is necessary to construct a feasible SMC. Firstly, the state variables of the DSPM machine should be defined as the Eq. (9).

$$\begin{cases} x_1 = x_{ref} - x \\ x_2 = \int_0^t x_1 dt = \int_0^t (x_{ref} - x) dt \end{cases} \quad (9)$$

Where: x_{ref} is the reference value; x is the actual measurement.

$$x_{ref} = [\omega_{mref} \quad i_{dref} \quad i_{qref}]^T, \quad x = [\omega_m \quad i_d \quad i_q]^T \quad (10)$$

Next, the sliding surface is designed under the utilization of system variables x_1 and x_2 as shown in the Eq. (11).

$$s = cx_2 + x_1 \quad (11)$$

Then, the derivation of the Eq. (11) can be obtained in the following Eq. **Error!**

Reference source not found. in combination with the Eqs. (5)-(9).

$$\begin{cases} \dot{s}_\omega = -\frac{1}{J_m} [T_{em} + T_m - B\omega_m] + cx_{1\omega} \\ \dot{s}_{i_d} = -\frac{1}{L_d} [v_d - (R_s + 2\omega_e M_{dq})i_d - M_{dq} \frac{di_q}{dt} + \omega_e (1.5L_d - 0.5L_q)i_q] + cx_{1d} \\ \dot{s}_{i_q} = -\frac{1}{L_q} [v_q - \sqrt{\frac{3}{2}}\varphi_1\omega_e - (R_s - 2\omega_e M_{dq})i_q - M_{dq} \frac{di_d}{dt} - \omega_e (1.5L_q - 0.5L_d)i_d] + cx_{1q} \end{cases} \quad (12)$$

Where: s_ω , s_d and s_q are sliding mode surfaces of the speed and current controllers respectively; $x_{1\omega}$, x_{1d} and x_{1q} are the tracking errors of the speed and current controllers respectively.

It is also essential to set up an initial integral value which is given in the Eq. (13).

The system trajectory can be quickly transferred to the sliding surface ($s = 0$) even at the

initial time ($t = 0$) under the action of I_0 . It means that the control system has global robustness.

$$I_0 = \int_{-\infty}^0 x_1(\tau) dt = -\frac{x_0}{c} \quad (13)$$

Where: c is a positive number; x_0 is the initial value of x_1 .

The control objective is to make the system state reach the sliding surface ($s(x, t) = 0$) in a finite time and has a second-order sliding mode ($\dot{s} = s = 0$). Therefore, some assumptions must be satisfied:

Case 1: u is bounded and continuous; for any virtual value of t , the system is steady;

Case 2: $\|f(x)\|_2 \leq F, \|g(x)\|_2 \leq G, F \in \mathbf{R}^n, G \in \mathbf{R}^n, \frac{\partial}{\partial u}[\dot{s}] > 0$.

When the system satisfies the above conditions, it is necessary to assume global boundedness of uncertainty. Thus, positive real numbers, including C, K_m and K_M , must meet the respective ranges as shown in the formula (14).

$$\begin{cases} |A| \leq C, A(x, t) = \frac{\partial}{\partial x}[\dot{s}][f(x) + g(x)u] \\ 0 < K_m < B < K_M, B(x, t) = \frac{\partial}{\partial u}[\dot{s}] \end{cases} \quad (14)$$

The following controllable first-order system is considered to replace the error tracking system of the direct and quadrature axes currents.

$$\dot{x} = u(t) + \xi(t) \quad (15)$$

Where: x is the state value of the current errors in direct and quadrature axes; $\xi(t)$ is the uncertain disturbance term of the system; $u(t)$ is the super-twisting control law [29].

Conventionally, the control law can be defined in the Eq. .

$$\begin{cases} u(t) = u_1(t) + u_2(t) \\ u_1(t) = -\beta |s|^{\frac{1}{2}} \text{sign}(s) \\ \dot{u}_2(t) = -\alpha \text{sign}(s) \end{cases} \quad (16)$$

Where: $\text{sign}(s)$ is the symbolic function; α and β are positive real numbers.

Actually, HOSMC based on STA is difficult to prove its system stability. Moreover, the relative controller parameters are difficult to determine due to uncertain

boundaries. Fortunately, HOSMC can further weaken the chattering theoretically and converge in a limited time under certain conditions. It only requires the sliding mode variable s and the suitable systems with a relative order of 1. Furthermore, because of positive gain parameters of the super-twisting control law, the restrictive conditions of α and β in the Eq. (18) should also be satisfied [30].

$$\begin{cases} \alpha > \frac{C}{K_m} \\ \beta^2 > 2 \frac{\alpha K_M + C}{K_m} \end{cases} \quad (17)$$

According to the description, the structure diagram of STA is shown in Fig. 4.

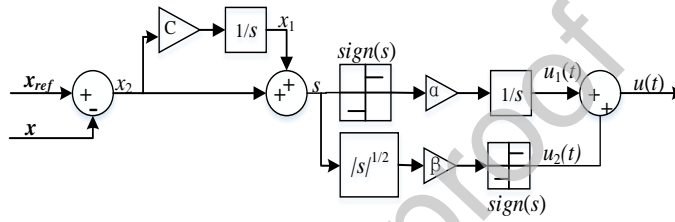


Fig. 4. STA structure diagram.

In the two-dimensional plane coordinated by s and \dot{s} , the uncertain state trajectory can spirally converge to the origin stable state within a finite time. The derivative formula of the sliding surface s established according to the formula **Error! Reference source not found.**, combined with Eqs. (15)-, the electromagnetic torque and voltage are obtained as below.

$$\begin{cases} T_{em} = J_m \left[\int \alpha_0 \text{sign}(s_\omega) dt + \beta_0 |s_\omega|^{\frac{1}{2}} \text{sign}(s_\omega) + \zeta_\omega(t) \right] + f\omega_m - T_m \\ v_d = L_d \left[\int \alpha_1 \text{sign}(s_d) dt + \beta_1 |s_d|^{\frac{1}{2}} \text{sign}(s_d) + \zeta_d(t) \right] + (R_s + 2\omega_e M_{dq}) i_d - \omega_e (1.5L_d - 0.5L_q) i_q + M_{dq} \frac{di_q}{dt} \\ v_q = L_q \left[\int \alpha_2 \text{sign}(s_q) dt + \beta_2 |s_q|^{\frac{1}{2}} \text{sign}(s_q) + \zeta_q(t) \right] + (R_s - 2\omega_e M_{dq}) i_q + \omega_e (1.5L_q - 0.5L_d) i_d + M_{dq} \frac{di_d}{dt} + \sqrt{\frac{3}{2}} \varphi_1 \omega_e \end{cases} \quad (18)$$

3.2 Stability based on improved HOSMC

Although HOSMC has obvious advantages, it still **ineluctably** produces chattering that worsens the system reliability and safety. It is worth noting that according to the formula, the traditional control law will bring contradictory phenomena. Once the speed towards to the sliding surface is accelerated, the convergence speed is also

increased, while the chattering will be also **increased dramatically**. Conversely, the **chattering and convergence speeds will be greatly reduced with the reduced speed to the sliding surface**. Consequently, it's very important to establish a reasonable control law to balance the chattering and convergence speeds when the point is not on the sliding **mode surface**. In order to solve this problem, the saturation function is proposed instead of the ideal symbol function to further reduce the chattering for this non-linear system. **Compared with the sign function**, this function will make the velocity gradually decrease to zero when it approaches the switching planes. The expression of the saturation function $\text{sat}(s)$ is shown in the Eq. (19). **Actually, it is a switching control outside the boundary layer and a linear feedback control inside the boundary layer.**

$$\text{sat}(s) = \begin{cases} 1, & s > \Delta \\ ks, & |s| \leq \Delta, k = \frac{1}{\Delta} \\ -1, & s < -\Delta \end{cases} \quad (19)$$

Where: Δ is boundary layer.

Accordng to this equation, the Eq. (18) can be rewritten with this substitution function.

$$\begin{cases} T_{em} = J_m \left[\int \alpha_0 \text{sat}(s_\omega) dt + \beta_0 |s_\omega|^{\frac{1}{2}} \text{sat}(s_\omega) + \xi_\omega(t) \right] + f \omega_m - T_m \\ v_d = L_d \left[\int \alpha_1 \text{sat}(s_d) dt + \beta_1 |s_d|^{\frac{1}{2}} \text{sat}(s_d) + \xi_d(t) \right] + (R_s + 2\omega_e M_{dq}) i_d - \omega_e (1.5L_d - 0.5L_q) i_q + M_{dq} \frac{di_q}{dt} \\ v_q = L_q \left[\int \alpha_2 \text{sat}(s_q) dt + \beta_2 |s_q|^{\frac{1}{2}} \text{sat}(s_q) + \xi_q(t) \right] + (R_s - 2\omega_e M_{dq}) i_q + \omega_e (1.5L_q - 0.5L_d) i_d + M_{dq} \frac{di_d}{dt} + \sqrt{\frac{3}{2}} \varphi_f \omega_e \end{cases} \quad (20)$$

Then, the system model is further simplified and the system state quantity y is constructed. **In practice, it is necessary to assume the absolute value of the system uncertain term not exceed an upper limit**. Therefore, a constant value can be set to make the first derivative zero. Ultimately, the Eq. (15) is transformed into the Eq. (21).

$$\begin{cases} \dot{x} = -\beta |x|^{\frac{1}{2}} \text{sat}(s) + y, & y = \xi(t) - \int_0^t \alpha \text{sat}(s) d\tau \\ \dot{y} = -\alpha \text{sat}(s) \end{cases} \quad (21)$$

In order to demonstrate the stability of whole system, it only needs to verify the deviation system can converge to the origin in a finite time. It means that the equation $\dot{x} = Ax$ must work. Thus, a matrix A needs to be set for the confirmation. The proof process is simply summarized as follows.

Firstly, let $A = \begin{bmatrix} -\frac{\beta}{2} & \frac{1}{2} \\ -\alpha & 0 \end{bmatrix}$. On the basis of its characteristic polynomial, the matrix

A is a Hurwitz matrix. Therefore, for any positive definite symmetric matrix Q , there exist a positive definite symmetric matrix P which must satisfy the following Lyapunov condition (22).

$$A^T P + PA = -Q \quad (22)$$

Secondly, a non-smooth quadratic-like function is chosen as the alternative Lyapunov function, which is defined as the Eq. (23) [33][34].

$$V(x, y) = \varepsilon^T P \varepsilon, \quad \varepsilon^T = [\varepsilon_1 \quad \varepsilon_2]^T = [|x|^{\frac{1}{2}} \text{sign}(x) \quad y] \quad (23)$$

Meanwhile, it is noteworthy that the function V is not only continuous positive definite but also radially unbounded. Except for the point set $\{x=0\}$, V is divisible everywhere. When the system does not converge to the origin, the system state does not always stay at a certain point of the set $\{x=0\}$ [31][32]. Then, let the derivative of V be \dot{V} , thus:

$$\dot{V} = \frac{1}{|\varepsilon_1|} \varepsilon^T (A^T P + PA) \varepsilon = -\frac{1}{|\varepsilon_1|} \varepsilon^T Q \varepsilon \quad (24)$$

Since the Lyapunov function V is a quadratic positive definite function, there are:

$$\lambda_{\min}(P) \|\varepsilon\|_2^2 \leq \varepsilon^T P \varepsilon \leq \lambda_{\max}(P) \|\varepsilon\|_2^2 \quad (25)$$

Where: $\lambda_{\min}(P)$ and $\lambda_{\max}(P)$ are the minimum and maximum eigenvalues of the positive definite symmetric matrix P ; $\|\cdot\|_2$ represents the 2-norm in the Euclid space \mathbf{R}^2 .

With $\|\varepsilon\|_2^2 = \varepsilon_1^2 + \varepsilon_2^2 = |x| + y^2$, hence,

$$|\varepsilon_1| = |x|^{1/2} \leq \|\varepsilon\|_2 \leq \frac{V^{1/2}}{\lambda_{\min}^{1/2}(\mathbf{P})} \quad (26)$$

$$\dot{V} \leq -\frac{1}{|\varepsilon_1|} \lambda_{\min}(\mathbf{Q}) \|\varepsilon\|_2^2 V \leq -\lambda_{\min}(\mathbf{Q}) \|\varepsilon\|_2 \leq -\zeta(\mathbf{Q}) V^{1/2}(x, y), \quad \zeta(\mathbf{Q}) = \frac{\lambda_{\min}(\mathbf{Q})}{\lambda_{\max}(\mathbf{Q})} \quad (27)$$

Finally, this is a constant who depends on the control law parameter (λ, α) and the matrix \mathbf{Q} . From Lyapunov's comparison theorem, the following inequality (28) is established [35].

$$t \geq \frac{2}{\zeta(\mathbf{Q})} V^{1/2}(x_0, y_0), V = 0 \quad (28)$$

That is to say, the system can stabilize to the origin within a limited time, and its convergence time can be estimated.

4. SIMULATION AND ANALYSIS

After the establishment of the control model, a double closed-loop simulation model based on MATLAB/Simulink was built to demonstrate the validity of the HOSMC. Moreover, the decoupling method was also applied in the model to reduce the complexity of the control system. The control strategy block diagram of the whole MCECS is shown in Fig. 5. The speed controller aims to achieve the maximum power from the marine current. The current controllers are to follow the expected quasi-sinusoidal current waveform perfectly to reduce the torque ripple. The relevant parameters of MCECS are shown in TABLE I.

In the previous work [23] and [34], various simulation results have verified that, this toothed pole DSPM machine still has larger torque ripple even with the conventional sinusoidal current. Therefore, one special current waveform called quasi-sinusoidal current is proposed to decrease the torque ripple. The definition of this current waveform is simplified in Appendix A, which is not elaborated in detail here.

changes to 3.0 m/s. The value of the d-axis current control error can also be stabilized to $[-0.5, 1]$. Fig. 6. B shows the variations of the q-axis current.

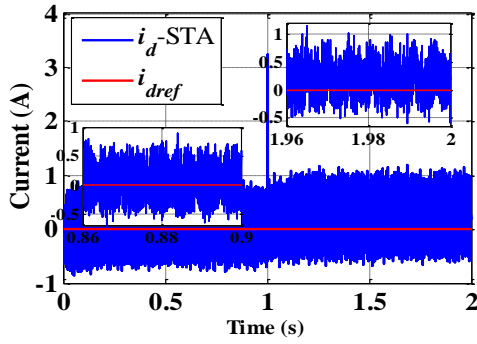


Fig. 6. A D-axis current

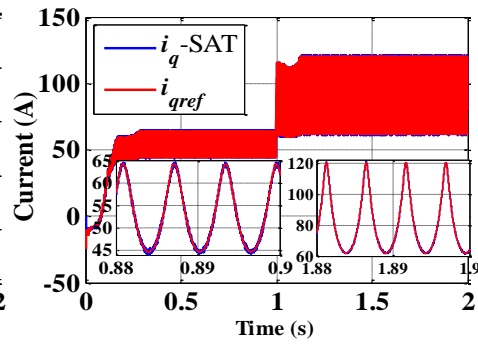


Fig. 6. B Q-axis current

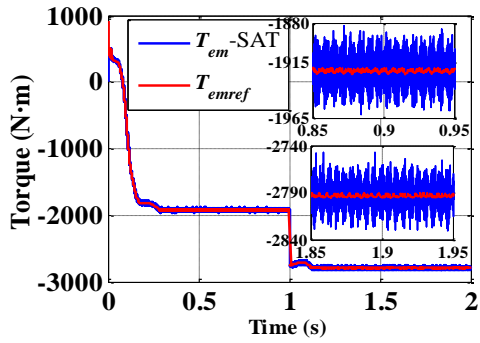


Fig. 6. C Electromagnetic torque

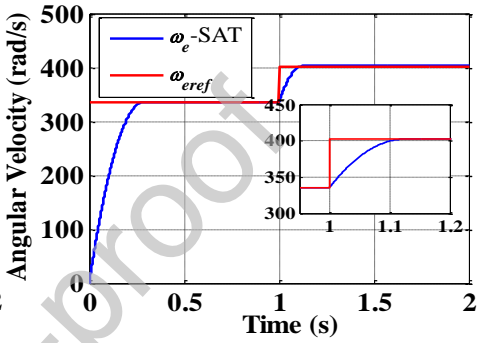


Fig. 6. D Electrical angular velocity

Fig. 6. Verification of STA-based HOSMC

Unlike the conventional sinusoidal current waveform, the q-axis current through coordinate transformation is not constant **due to the desired harmonic terms**. Fortunately, with the STA-based HOSMC, such current component can also **be** accurately tracked. For the variation of electromagnetic torque in Fig. 6. C, the electromagnetic torque has a certain overshoot inevitably in the start-up stage. The tracking error of electromagnetic torque can be controlled within 2.0 % when it reaches the stable state in the first stage. Once the ocean current velocity V_{tide} suddenly changes to 3.0 m/s, the electromagnetic torque can be adjusted perfectly in a relatively short time. By comparing the torque ripple, it is found that the tracking error is smaller. As the electrical angular velocity of the machine is proportional to the mechanical angular velocity, the change of the electrical angular velocity reflects the mechanical angular velocity. Fig. 6. D shows that the tracking error of electrical angular velocity is far less than 1 %.

4.2 Testing the robustness of STA

Actually, SMC is highly favored owing to its robustness and good dynamic performance. Hence, the main emphasis is always placed on proof of the robustness. In this section, the parameters of the machine will be changed to verify the robustness of the controllers. If the machine can still resume stable operation in a limited time when the parameters change, it is considered to be robust.

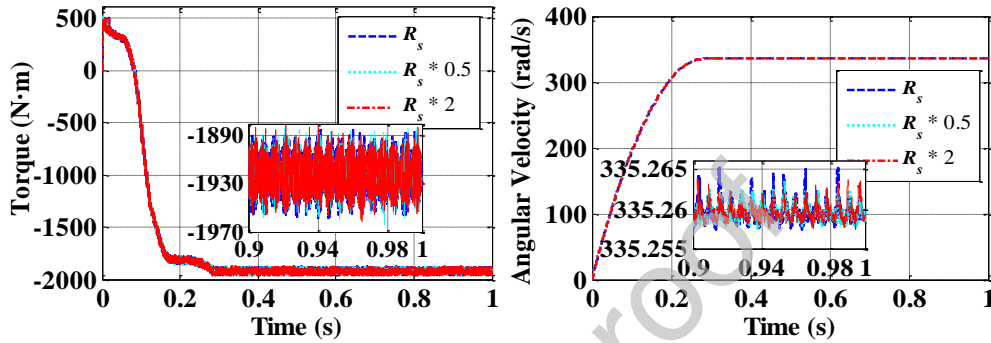


Fig.7. A Electromagnetic torque. Fig.7. B Electromagnetic angular velocity.

Fig. 7. Influence of R_s .

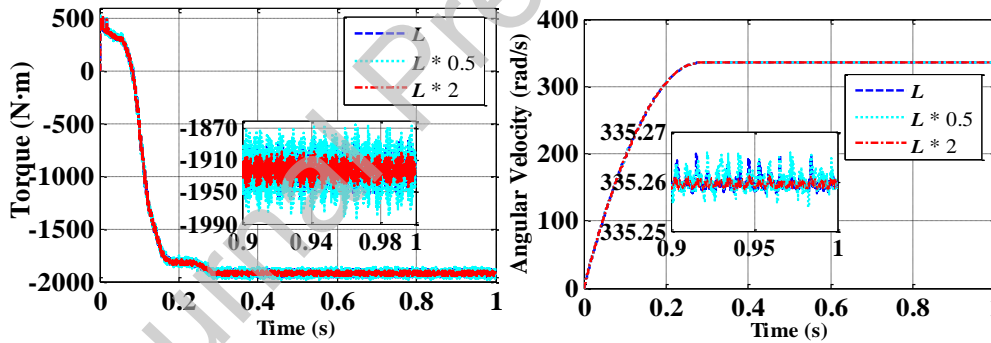


Fig. 8. A Electromagnetic torque.

Fig. 8. B Electrical angular velocity.

Fig. 8. Influence of L

The operation of the overall system was tested under different multiples of the stator resistance R_s and inductance L . The values of R_s and L in the machine model will be changed from 50% to 200% of the initial value with other constant parameters. The electromagnetic torque and electrical angular velocity are selected and shown in Fig. 7 and Fig. 8 consequently. In order to facilitate the simulation, the marine current velocity is given as a fixed value. The red lines indicate that the stator resistance or inductance is twice the original value. Similarly, the cyan lines indicate that the parameter is half of the original value.

From Fig.7. A and Fig.7. B, STA-based HOSMC can still approach the reference at the same response time and track the reference well with the great variation of the resistance R_s . Evidently, the changes in both electrical angular velocity and electromagnetic torque caused by the variation in resistance is negligible. From the other two pictures in Fig. 8. A and Fig. 8. B, the results equally illustrate that there is only slight distinction generated by the inductance variation. According to the simulation results, they can well validate the robustness to the significant variation of parameters under the STA-based HOSMC.

5. CONCLUSION

This paper mainly studies the control strategy for the DSPM machine, which is used for direct drive MCECS. Firstly, the turbine model is established. Under the SHOM method, a practical first-order marine current resource model is obtained. Then, a STA-based HOSMC is firstly proposed to control the speed and current of the DSPM machine. The integral sliding surface and control law are well designed and improved subsequently. Meanwhile, a quadratic Lyapunov function is used to prove the stability of the system within a limited time. According to the simulation results, not only the effective control under the variable marine current velocity but also the strong robustness with different machine parameters are verified. However, although the control effect has been greatly improved, the parameters of the controller are fixed and cannot be changed as the control parameters change. Therefore, it is meaningful to combine the intelligent algorithm to obtain the real-time optimal solution of controller parameters.

Acknowledgments

This work was supported by National Natural Science Foundation of China, China (Grant No: 61503242) and Natural Science Foundation of Shanghai, China (15ZR1419800).

Appendix A

The quasi-sinusoidal current in a three-phase stationary coordinate system is shown in Eq. (A.1):

$$\begin{cases} i_a = -I_m(\theta_e) \sin(\theta_e + \theta_0) \\ i_b = -I_m(\theta_e) \sin(\theta_e - \frac{2\pi}{3} + \theta_0) \\ i_c = -I_m(\theta_e) \sin(\theta_e + \frac{2\pi}{3} + \theta_0) \end{cases} \quad (\text{A.1})$$

Where: $I_m(\theta_e)$ is quasi-sinusoidal current amplitude, which varies with electrical angle θ_e .

Meanwhile, the formula of the basic electromagnetic torque can be rewritten as follows:

$$T_{em} = -[\frac{3}{2} N_r \varphi_1 \cos \theta_0 I_m(\theta_e) + \frac{3}{4} N_r (\frac{1}{2} L_1 + M_1) \sin(3\theta_e + 2\theta_0) I_m^2(\theta_e)] \quad (\text{A.2})$$

Because the current has to be some actual value in theory, the amplitude of this current is shown in the Eq. (A.3).

$$I_m(\theta_e) = \frac{-\frac{3}{2} N_r \varphi_1 \cos \theta_0 + \sqrt{(\frac{3}{2} N_r \varphi_1 \cos \theta_0)^2 - 3 N_r (\frac{1}{2} L_1 + M_1) \sin(3\theta_e + 2\theta_0) T_{em}}}{\frac{3}{2} N_r (\frac{1}{2} L_1 + M_1) \sin(3\theta_e + 2\theta_0)} \quad (\text{A.3})$$

References

- [1] H. Chen, T. Tang, N. Aït-Ahmed, M. E. H. Benbouzid, M. Machmoum and M. E. Zaïm, Attraction, challenge and current status of marine current energy, IEEE Access 6 (2018) 12665-12685.
- [2] M. Benbouzid, J.A. Astolfi, Marine Renewable Energy Handbook, in B. Multon, Concepts, modeling and control of tidal turbines, John Wiley & Sons, London, UK: ISTE; Hoboken, USA, 2012, pp. 219-278.
- [3] Z. Zhou, M. Benbouzid, J. Charpentier, Jean-Frédéric, F. Scuiller, T. Tang, Developments in large marine current turbine technologies-A review, Renewable and Sustainable Energy Reviews. 71 (2017) 852-858.

- [4] Statistical Review of World Energy,
<https://www.bp.com/en/global/corporate/energy-economics/statistical-review-of-world-energy.html>, accessed April 2019.
- [5] Renewables Global Status Report, REN21, 2017 (accessed 28 October 2019).
https://www.ren21.net/wp-content/uploads/2019/05/GSR2017_Full-Report_English.pdf
- [6] A.G.L. Borthwick, Marine Renewable Energy Seascape, *Engineering*, 2(1) (2016) 69-78.
- [7] E. Ozkop, I.H. Atlas, Control, power and electrical components in wave energy conversion systems: A review of the technologies, *Renewable and Sustainable Energy Reviews*. 67 (2017) 106-115.
- [8] M. Leijon, K. Nilsson, Direct electric energy conversion system for energy conversion from marine currents, *Proceedings of the Institution of Mechanical Engineers, Part A: Journal of Power and Energy*. 221(2) (2007) 201-205.
- [9] H. Chen, T. Tang, Jin. Han, Ait-Ahmed, Nadia, M. Machmoum, Zaim, E. Mohammed, Current waveforms analysis of toothed pole Doubly Salient Permanent Magnet (DSPM) machine for marine tidal current applications, *International Journal of Electrical Power & Energy Systems*. 106 (2019) 242-253.
- [10] K.T Chau, M. Cheng, C. Chan, Performance analysis of 8/6-pole doubly salient permanent magnet motor, *Electric Machines and Power Systems*. 27(10) (1999) 1055-1067.
- [11] K.T. Chau, Q. Sun, Fan, Y., M. Cheng, Torque ripple minimization of doubly salient permanent magnet motors, *IEEE Transactions on Energy Conversion*. 20(2) (2005) 352-358.
- [12] X. Meng, X. Pang, Wang H., Analysis of Angle-advance control doubly salient Electro-magnetic motor, *Journal of Nanjing University of Aeronautics & Astronautics (in Chinese)*. 36(5) (2004) 623-627.
- [13] Q. Hu, Y. Yan, Prior angle control for doubly salient permanent magnet motor, *Transactions of China Electro technical Society (in Chinese)*. 20(9) (2005) 13-18.
- [14] Q.J. Z, D. Liang, P. Kou and Z. Liang, Dual closed-loop control of a doubly salient permanent magnet generator based on gain-scheduling PI controller, 2017 IEEE International Electric Machines and Drives Conference (IEMDC). (2017) 1-8.

- [15] H. Chen, N. Ait-Ahmed, M. Machmoum, and E. H. Zaim, Modeling and Vector Control of Marine Current Energy Conversion System Based on Doubly Salient Permanent Magnet Generator, *IEEE Transactions on Sustainable Energy*. 7(1) (2016) 409-418.
- [16] Free stock photos-Pexels,
https://cdn.pixabay.com/photo/2016/01/19/15/08/ocean-wave-1149174__340.jpg, accessed April 2019.
- [17] Atlantis Resources Corporation, <http://atlantisresourcesltd.com>, accessed April 2019.
- [18] S. Benelghali, On multiphysics modeling and control of marine current turbine systems, Ph.D. dissertation, Dept. Elect. Eng., Université de Bretagne Occidentale, Brest (2009).
- [19] S. J. Couch, I. Bryden, Tidal current energy extraction: hydrodynamic resource characteristics, *Proceedings of the Institution of Mechanical Engineers, Part M: Journal of Engineering for the Maritime Environment*. 220(4) (2006) 185-194.
- [20] A.S. Bahaj, L.E. Myers, Fundamentals applicable to the utilization of marine current turbines for energy production, *Renewable Energy*. 28(14) (2003) 2205-2211.
- [21] R. Saou, M. E. Zaïm, K. Alitouche, Optimal Designs and Comparison of the Doubly Salient Permanent Magnet Machine and Flux-reversal Machine in Low-speed Applications, *Electric Power Components and Systems*. 36(9) (2008) 914-931.
- [22] Torrey, D.A, M. Hassanin, The design of low-speed variable-reluctance generators, *IEEE Industry Applications Conference*. 1(1) (1995) 8-12.
- [23] H. Chen, N., Ait-Ahmed, L. Moreau, M. Machmoum, and M. E. Zaim, Performances analysis of a Doubly Salient Permanent Magnet Generator for marine tidal current applications, *Power Electronics & Application Conference & Exposition*. (2015) 320-325.
- [24] A. Levant, Higher Order Sliding Modes, Differentiation and Output-Feedback Control, *International Journal of Control*. 76(9/10) (2003) 924-941.
- [25] **Chaos, Solitons & Fractals, Fitted fractional reproducing kernel algorithm for the numerical solutions of ABC-Fractional Volterra integro-differential equations. 126 (2019) 394-402.**
- [26] **Chaos, Solitons & Fractals, Modulation of reproducing kernel Hilbert space method for numerical solutions of Riccati and Bernoulli equations in the Atangana-Baleanu fractional sense. 125 (2019) 163-170**

- [27] S. Benelghali, M. Benbouzid, J.F. Charpentier, T. Ahmed-Ali, I. Munteanu, Experimental Validation of a Marine Current Turbine Simulator: Application to a Permanent Magnet Synchronous Generator-Based System Second-Order Sliding Mode Control, *IEEE Transactions on Industrial Electronics*, Institute of Electrical and Electronics Engineers. 58(1) (2011) 119-126.
- [28] S. Benelghali, M. Benbouzid, T. Ahmed-Ali, J.F. Charpentier, High-Order Sliding Mode Control of a Marine Current Turbine Driven Doubly-Fed Induction Generator, *IEEE Journal of Oceanic Engineering*, Institute of Electrical and Electronics Engineers. 35(2) (2010) 402-411.
- [29] A. Levant, Robust exact differentiation via sliding mode technique, *Automatica*. 4(3) (1998) 379-384.
- [30] A. Levant, Principles of 2-Sliding Mode Design, *Automatica*. 43(4), (2007) 576-586.
- [31] *Chaos, Solitons & Fractals*, Atangana-Baleanu fractional approach to the solutions of Bagley-Torvik and Painlevé equations in Hilbert space. 117 (2018) 161-167.
- [32] *Chaos, Solitons & Fractals*, Numerical solutions of integrodifferential equations of Fredholm operator type in the sense of the Atangana-Baleanu fractional operator. 117 (2018) 117-124
- [33] A.M. Jaime, O. Marisol, A Lyapunov Approach to Second Order Sliding Mode Controllers and Observers, *Proceedings of the IEEE International Conference on Decision and Control*. New York, USA, (2008) 2856-2861.
- [34] A. Dávila, J. A. Moreno and L. Fridman, Optimal Lyapunov function selection for reaching time estimation of Super Twisting algorithm, *Proceedings of the 48th IEEE Conference on Decision and Control (CDC) held jointly with 2009 28th Chinese Control Conference*, Shanghai. (2009) 8405-8410.
- [35] H.K. Khalil, H. Prentice, *Nonlinear Systems*, 3rd Ed, Upper Saddle River, New Jersey, (2010) 5109-511
- [36] H. Chen, N. Aït-Ahmed, M. Machmoum, M.E. Zaim, E. Schaeffer, Modeling and current control of a double salient permanent magnet generator (DSPMG). 2013 15th European Conference on Power Electronics and Applications (EPE), Lille, (2013) 1-10.

Declaration of interests

The authors declare that they have no known competing financial interests or personal relationships that could have appeared to influence the work reported in this paper.

Journal Pre-proof